Imaging of plasmacytoid dendritic cell interactions with T cells

*María Mittelbrunn,[1] *Gloria Martínez del Hoyo,[1] María López-Bravo,[2] Noa B. Martín-Cofreces,[3] Alix Scholer,[4] Stéphanie Hugues,[4] Luc Fetler,[5] Sebastián Amigorena,[5] Carlos Ardavín,[2] and Francisco Sánchez-Madrid[1,3]

[1]Departamento de Biología Vascular e Inflamación, Centro Nacional de Investigaciones Cardiovasculares, Madrid, Spain; [2]Departamento de Inmunología y Oncología, Centro Nacional de Biotecnología/Consejo Superior de Investigaciones Científicas, Madrid, Spain; [3]Servicio de Inmunología, Hospital de la Princesa, Universidad Autónoma de Madrid, Madrid, Spain; [4]INSERM Unite Mixte de Recherche 653, Immunité et Cancer, Pavillon Pasteur, Institut Curie, Paris, France; and [5]Centre National de la Recherche Scientifique, Unite Mixte de Recherche 168, Laboratoire de Physico-Chimie Curie, Institut Curie, Paris, France

Plasmacytoid dendritic cells (pDCs) efficiently produce type I interferon and participate in adaptive immune responses, although the molecular interactions between pDCs and antigen-specific T cells remain unknown. This study examines immune synapse (IS) formation between murine pDCs and CD4+ T cells. Mature pDCs formed canonical ISs, involving relocation to the contact site of the microtubule-organizing center, F-actin, protein kinase C-θ, and pVav, and activation of early signaling molecules in T cells. However, immature pDCs were less efficient at forming conjugates with T cells and inducing IS formation, microtubule-organizing center translocation, and T-cell signaling and activation. Time-lapse videomicroscopy and 2-photon in vivo imaging of pDC–T-cell interactions revealed that immature pDCs preferentially mediated transient interactions, whereas mature pDCs promoted more stable contacts. Our data indicate that, under steady-state conditions, pDCs preferentially establish transient contacts with naive T cells and show a very modest immunogenic capability, whereas on maturation, pDCs are able to form long-lived contacts with T cells and significantly enhance their capacity to activate these lymphocytes. (Blood. 2009;113: 75-84)

Introduction

Dendritic cells (DCs) are the most efficient antigen-presenting cells (APCs) because of their ability to capture, process, and present antigens to naive T lymphocytes.[1] DCs can be classified into 2 major categories: conventional DCs (cDCs), which in turn include different DC subsets, and plasmacytoid DCs (pDCs), which have emerged over the last few years as an important DC subset involved in both innate and adaptive immune responses.[2] In mice, pDCs can be identified as CD11c^{int}B220+ cells found in bone marrow, blood, thymus, and peripheral lymphoid organs.[3-5] These cells provide an initial defense mechanism against viral infection by producing large amounts of type I interferon (IFN) on recognition of viral nucleic acids through Toll-like receptors (TLR) 7 and 9. After exposure to maturation stimuli such as TLR-ligands or signals from activated T lymphocytes such as CD40L, pDCs can also act as APCs, participating in the induction of antigen-specific T-cell responses and activating other components of the immune system such as NK cells and B cells.[6] Growing evidence supports the essential role of pDCs in viral immunology,[7] inflammatory and autoimmune diseases,[8] and tolerance induction.[5,9,10] In steady state, pDCs display an immature phenotype characterized by low expression of major histocompatibility complex (MHC) class II and costimulatory molecules and a markedly limited T-cell stimulatory potential.[4] Reports demonstrating that immature DCs can induce T-cell tolerance against self-antigens[11] have led to proposals that pDCs might be involved in the maintenance of immunologic T-cell tolerance. This concept is supported by recent studies that addressed the tolerogenic role of pDCs both in vitro[5,9] and in vivo[10,12];

however, the mechanisms by which immature pDCs may exert a tolerogenic function remain unclear.

The initiation of an immune response involves initial transient DC–T-cell contacts that allow T cells to scan the DC surface for specific MHC-peptide ligands.[13] Once T cells have encountered their specific antigenic peptides, the DC–T-cell interaction is stabilized by the formation of a structure known as the immunologic synapse (IS). It has been described that the mature IS comprises 2 concentric supramolecular activation clusters (SMACs): a central SMAC (cSMAC), where antigen receptors and signaling molecules are located; and a surrounding peripheral SMAC (pSMAC), containing adhesion molecules and cytoskeletal elements.[14,15] In addition, it has been proposed that T-cell receptor (TCR) microclusters initially assemble at the pSMAC, where early phosphorylation events take place, and then move to converge in the cSMAC, where signaling is terminated by internalization and degradation of membrane receptors.[16]

We have analyzed the organization of the IS formed between pDC and T lymphocytes as well as its kinetics and their potential implications in the activation of T cells. By using immunofluorescence analysis, in vitro confocal time-lapse live videomicroscopy and intravital 2-photon microscopy, we found that mature pDCs were able to form long-lived canonical IS with CD4+ T cells. In contrast, immature pDCs mostly established short-lived contacts. In addition, whereas mature pDCs were able to efficiently induce the activation of T cells, immature pDCs showed a very limited immunogenic capability.

The online version of this article contains a data supplement.

Methods

Mice and DCs

C57BL/6, OT-II, C57BL/6 Ly5.1 Pep[3b], and UBI-GFP mice were bred under specific pathogen-free conditions, following European recommendations.

DCs were in vitro–differentiated from bone marrow in RPMI 1640 medium with 10% fetal bovine serum, 50 μM 2-mercaptoethanol, and 100 ng/mL Flt3-ligand (Flt3-L; PeproTech, Rocky Hill, NJ). Maturation was induced with cytosine-phosphate-guanosine (CpG) oligodeoxynucleotide-1826: TCCATGACGTTCCTGACGTT (24 hours, 6 μg/mL). pDCs and cDCs were isolated using an AUTOMACS sorter (Miltenyi Biotec, Auburn, CA). Splenic DCs and pDCs isolated ex vivo from lymph nodes were obtained as described.[5] Flow cytometric analyses were performed on a FACSCalibur flow cytometer (BD Biosciences, San Jose, CA). Institutional Review Board approval for the studies was obtained from the National Center of Cardiovascular Research.

T-cell stimulation assays

OT-II cells were cocultured with either immature or mature pDCs or cDCs (10:1 T cell/DC ratio; 10^5 cells/well; 72 hours) in the presence of ovalbumin (OVA) peptide and analyzed for cell proliferation and activation by ^{3}H-thymidine uptake (^{3}H-TdR, 1.0 μCi/well) and CD25 surface expression.

Conjugate formation and immunofluorescence assays

OT-II cells, loaded with chloromethyl aminocoumarin (5 μM, 30 minutes, 37°C; Invitrogen, Carlsbad, CA), were mixed with DCs (3:1 T-cell/DC ratio) with OVA peptide (10 μg/mL, 30 minutes; at 37°C), centrifuged, and incubated (37°C; 15 minutes or 2 hours). Cells were fixed for 5 minutes in 4% formaldehyde–phosphate-buffered saline and stained with phalloidin–Alexa 568 (Invitrogen), anti–α-tubulin–fluorescein isothiocyanate (FITC; Sigma-Aldrich, St Louis, MO), anti–phospho-Tyr174 Vav (pY174; from Dr X. Bustelo, Salamanca, Spain), anti-Arp2/3, anti–protein kinase C-θ (PKC-θ), and anti-Talin (Santa Cruz Biotechnology, Santa Cruz, CA) followed by secondary antibodies labeled with Rhodamine-X or Alexa 488 (Invitrogen). Ex vivo pDC conjugates were stained with anti–CD11c-FITC (BD PharMingen, San Diego, CA) and anti–PKC-θ, followed by Rhodamine-X.

Western blot

DCs (5×10^5) were mixed with OT-II cells (5×10^6), incubated (37°C, 15 minutes), and lysed; Western blot analysis was performed as previously described.[17] Results are expressed as the arithmetic mean plus or minus SD of the fold induction relative to the immature pDC condition.

Time-lapse fluorescence confocal microscopy

Coverslips were coated with fibronectin (20 μg/mL; Sigma-Aldrich), mounted in Attofluor open chambers (Invitrogen), and OVA peptide-preloaded DCs (2×10^5) were allowed to adhere for 30 minutes. OT-II T cells (6×10^5), incubated with calcein (5 μM; Invitrogen), were added, and the chambers were maintained at 37°C, 5% CO_2. Confocal images were acquired and processed as described for immunofluorescence assays.

Immunohistologic staining

Spleens were embedded in tissue freezing medium (OCT, Tissue-Tek; Sakura Finetek Europe, Zoeterwoude, The Netherlands) and flash frozen in liquid nitrogen; 5-μm cryosections were stained with anti–MOMA-1–biotin (BMA Biomedicals, Augst, Switzerland), anti-CD3–Alexa 647 (Invitrogen), Hoechst 33258 (Invitrogen), and anti–green fluorescent protein (GFP; Santa Cruz Biotechnology). Secondary antibodies were from Invitrogen.

Photon laser scanning microscopy

C57BL/6 recipients were injected intravenously with pDCs (8×10^6) from C57BL/6 GFP mice and, 24 hours later, with chloromethyl-benzoylaminotetramethylrhodamine (CMTMR)–labeled (5 μM, 30 minutes, 37°C; Invitrogen) OT-II T cells (12×10^6). After 4 hours, mice were anesthetized and the spleen surgically exposed on a coverslip for 2-photon imaging. Temperature was maintained at 37°C. The apparatus for time-lapse 2-photon laser-scanning microscopy consisted of a 20×/0.95 numeric aperture (NA) dipping objective (Olympus) fitted with a 555-nm dichroic mirror and mounted on an LSM510 Meta microscope (Carl Zeiss, Jena, Germany) coupled to a Maitai femtosecond laser (690-1020 nm; Spectra Physics, San Jose, CA). The excitation wavelength was 870 nm. Six images with 6-μm z-spacing were acquired every 30 seconds during 30 to 60 minutes.

Statistical analysis

Data were compared by the nonparametric Mann-Whitney U, Kruskal-Wallis, or χ^2 tests with an α value of 0.05.

Results

Conjugate formation between pDCs and CD4⁺ T cells

Flt3-L–driven mouse bone marrow cultures have been shown to generate 2 subpopulations of CD11c⁺ DCs, which can be defined according to their expression of B220 or CD11b.[18,19] CD11c⁺B220⁺CD11b⁻ DCs correspond to the in vitro counterparts of pDCs, whereas CD11c⁺B220⁻CD11b⁺ DCs are equivalent to cDCs. These DC subpopulations were isolated on the basis of their differential expression of B220 and CD11b (Figure S1, available on the *Blood* website; see the Supplemental Materials link at the top of the online article), and were induced to mature by stimulation with the TLR9-ligand CpG 1826. In the absence of maturation stimuli, Flt3-L–derived pDCs displayed a notable immature phenotype characterized by low surface expression of MHC class II and costimulatory molecules (Figure 1A). In contrast, immature cDCs expressed significantly higher levels of these molecules (Figure 1A). On CpG treatment, cDCs continued to express higher surface levels of MHC class II and costimulatory molecules than pDCs (Figure 1A). The expression levels of MHC class II and costimulatory molecules were also assessed in freshly isolated pDCs from lymph nodes. As shown in Figure S2 and Table S1, ex vivo–isolated pDCs expressed more surface MHC class II molecules than Flt3-L in vitro–derived immature pDCs, whereas the expression levels of costimulatory molecules were similar.

The capacity of OVA peptide–loaded pDCs to form stable conjugates with naive OT-II CD4⁺ T cells was assessed before and after CpG-induced maturation and compared with that of cDCs. For this, OT-II T cells were conjugated for 30 minutes with Flt3-L-derived DCs in the absence or in the presence of OVA peptide. In the presence of antigen, the capacity of immature pDCs to form stable conjugates with T cells was significantly lower, at 2 times of incubation tested, compared with mature pDCs or cDCs. In addition, the capacity of immature pDCs to form stable conjugates with T cells was not increased in the presence of antigen (Figure 1B). Likewise, the percentage of conjugates formed by ex vivo-isolated pDCs was similar in the absence or presence of OVA peptide (18% vs 22%). In contrast, the other DC subsets tested showed an enhanced capability to form stable conjugates on antigen addition (Figure 1B).

To determine whether differences in conjugate formation between pDCs and cDCs could be the result of distinct expression patterns of adhesion molecules, we analyzed the expression of
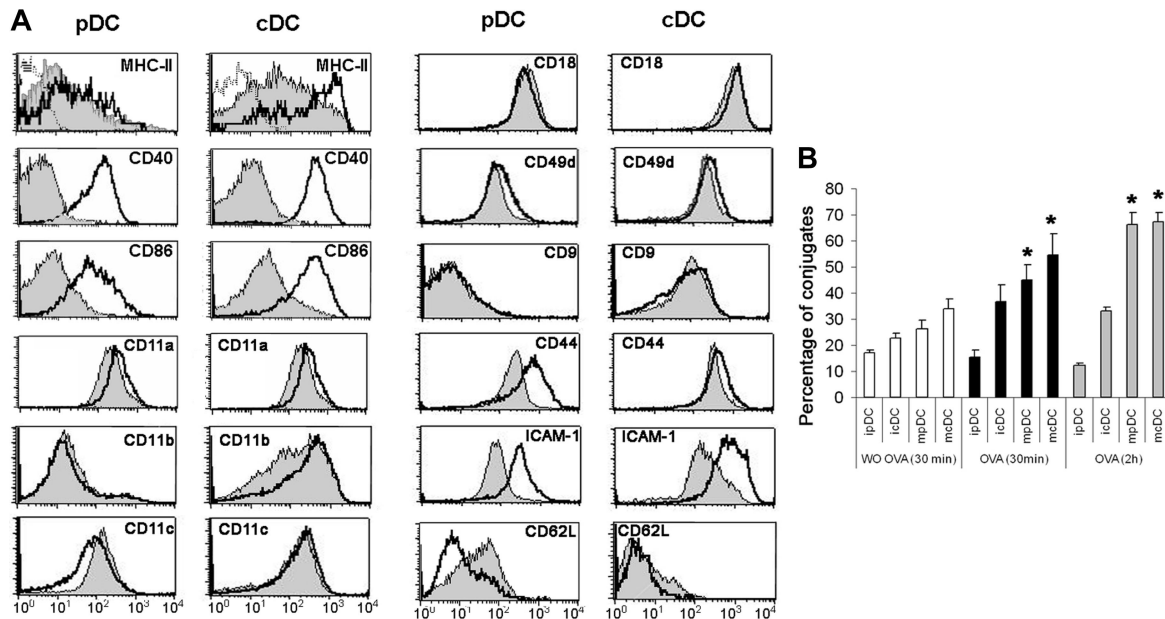
Figure 1. Conjugate formation capacity by pDCs and cDCs. (A) Expression of MHC class II, costimulatory and adhesion molecules by Flt3-L–derived immature and CpG-matured pDCs and cDCs. The phenotype of immature (gray histogram) or mature (white histogram) pDCs or cDCs was analyzed by 3-color flow cytometry. Dotted lines correspond to the negative control. (B) Immature or CpG-matured pDCs and cDCs were conjugated with OT-II CD4$^+$ T cells either in the absence (□) or presence of OVA peptide (10 μg/mL) at 30 minutes (■) or 2 hours (▨). Cells were allowed to adhere to poly-L-lysine (PLL) and fixed. Results are expressed as the percentage of DCs forming conjugates with T lymphocytes. Data represent the arithmetic mean plus or minus SEM of 5 experiments. ipDC indicates immature pDCs; mpDC, mature pDCs; icDC, immature cDCs; mcDC, mature cDCs. *$P <$ .05 compared with ipDCs.

adhesion molecules and the tetraspanin CD9 on immature and mature pDCs and cDCs by flow cytometry (Figure 1A). Besides confirming the reported differences in integrin α_M (CD11b, Mac1) and CD62L (L-selectin) expression, which are used to define cDC and pDC subpopulations, this analysis revealed a notable contrast between the absence of the tetraspanin CD9 from in vitro–differentiated and ex vivo–isolated pDCs and its high expression on cDCs (Figures 1A, S2). Tetraspanins laterally associate with several surface receptors, including integrins and MHC class II,[20] and it has also been described that CD9 promotes the formation of MHC class II multimers and enhances antigen presentation,[21] although the role of tetraspanins facilitating T-APC conjugation has not been addressed yet. In addition, pDCs (mainly immature and freshly isolated cells) showed a diminished expression of the α_4 integrin chain (CD49d), CD44, and intercellular adhesion molecule 1 (ICAM-1; Figures 1A,S2). All these data indicate that immature pDCs show a diminished capability to form stable conjugates with T lymphocytes, and suggest that this phenomenon could be related to a defective expression of different adhesion molecules.

pDCs can form canonical immune synapses with CD4$^+$ T cells

We next addressed whether pDCs can form ISs with naive T lymphocytes and how these synapses compare with those formed by cDCs. This was done by analyzing several characteristic IS markers on OVA peptide-loaded pDC–OT-II CD4$^+$ T-cell conjugates. Staining of F-actin and the Arp2/3 complex showed actin cytoskeleton polymerization at the contact zone during immature or mature pDC–T-cell interactions, forming a ring structure characteristic of the pSMACs (Figures 2A,S3B). Talin was also localized at the pSMAC of pDC and cDC ISs (Figure S3A).

During cognate interactions of conventional DCs with T lymphocytes, the T-cell microtubular cytoskeleton undergoes dramatic changes that lead to a reorientation of the microtubule-organizing center (MTOC) toward the vicinity of the DC–T-cell contact area.[22] To determine whether pDCs can induce such

cytoskeletal rearrangements during pDC–T-cell interactions, we prepared conjugates of naive OT-II T cells with OVA peptide-loaded mature cDCs and pDCs, and double-stained them for α-tubulin and CD11b to identify the MTOC and to mark cDCs, respectively. Both DC subsets induced T-cell MTOC translocation toward the contact zone (Figure 2B). To further confirm that MTOC translocation to the IS was induced by pDCs, we stained for α-tubulin in conjugates formed between CD4$^+$ T cells and purified mature pDCs (Figure 2C bottom panel). Interestingly, quantitative analysis of MTOC translocation in T cells forming stable conjugates with DCs revealed that, whereas mature pDCs actively induced MTOC translocation to the contact zone in the presence of OVA peptide (Figure 2D), immature pDCs were unable to do so (Figure 2C top panel, 2D). In contrast, the capacity of cDCs to induce MTOC translocation on CD4$^+$ T cells did not differ significantly before and after maturation (Figure 2D).

T-cell signaling and activation induced by pDCs

TCR engagement induces the phosphorylation and relocation of specific signaling components that interact with the TCR-CD3 complex. To study the signaling events triggered by pDCs during IS formation, we analyzed 2 markers of T-cell activation: phosphorylation of the Rac-1 regulator Vav-1 and the relocation of PKC-θ to the contact zone. Phosphorylation of the adaptor molecule Vav-1 at Tyr 147, a modification essential for its activation, was frequently observed at the contact zone between mature pDCs and OT-II CD4$^+$ T cells, whereas it was scarcely detected in T-cell conjugates formed with immature pDCs (Figure 3A left panel). PKC-θ was also observed concentrated at the contact zone, with translocation detected in approximately 50% of ISs induced by mature OVA-loaded pDCs. This percentage diminished to approximately 20% in immature pDC–T-cell conjugates (Figure 3A right panel, 3B). By comparison, immature cDCs induced PKC-θ translocation to a similar extent as mature pDCs, and mature cDCs were highly efficient inducers (Figure 3B). Ex vivo–isolated pDCs induced a
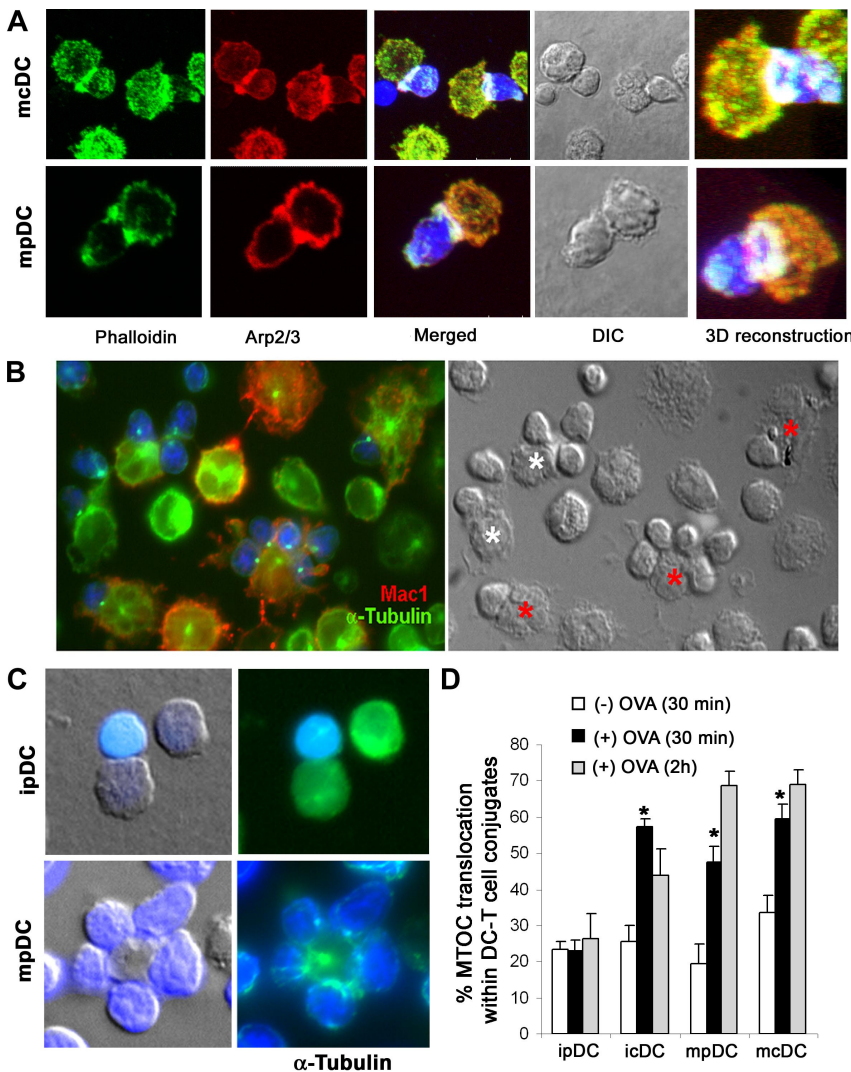
Figure 2. pSMAC formation and MTOC reorientation in pDC–T-cell conjugates. (A) pSMACs formed between OVA peptide–loaded mature pDCs (mpDC) and cDCs (mcDC) and blue-labeled OT-II CD4⁺ T cells. Plates show the maximal projection of confocal images from pDC and cDC ISs stained with phalloidin (green) and Arp2/3 (red), the differential interference contrast image, and a high magnification 3-dimensional reconstruction of the pSMAC. For Figures 2A, 3C, 5A, 6D, and S3A-C, a Leica TCS-SP5 confocal laser scanning unit attached to a Leica DMI6000 inverted epifluorescence microscope, with a HCX PL APO 63×/1.40-0.6 NA oil was used. Images were acquired with Leica confocal software, and figures were composed with Adobe Photoshop CS. (B) Matured Flt3-L–derived cells (mpDCs and mcDCs) were loaded with OVA peptide and conjugated with blue-labeled OT-II CD4⁺ T cells and double-stained for CD11b (red) and α-tubulin (green). cDCs and pDCs are indicated by red and white asterisks, respectively. For Figures 2B, 2C, and 3A, fixed cells were mounted on ProLong Gold (Invitrogen) and observed at 22°C on a Leica DMR photomicroscope (Leica, Wetzlar, Germany) with a HCX PL APO 63×/1.32-0.6 NA oil objective, coupled to a COHU 4912-5010 Camera (COHU, San Diego, CA). The acquisition software was Leica QFISH, version 2.1, and images were processed with Adobe Photoshop CS. (C) Immature and mature pDCs were conjugated with blue-labeled OT-II CD4⁺ T cells and stained for α-tubulin (green). (D) Estimation of MTOC translocation on conjugates formed between immature or mature pDCs or cDCs and OT-II CD4⁺ T cells either in the absence or presence of OVA peptide. Results are presented as the percentage of conjugates in which the MTOC was translocated to the IS. Data are arithmetic mean plus or minus SEM of 5 experiments. *$P < .05$ compared with the absence of antigen (Kruskal-Wallis test).

similar level of PKC-θ translocation in T-cell conjugates as Flt3-L in vitro–derived immature pDCs, with translocation detected in approximately 10% of ISs induced by ex vivo OVA-loaded pDCs (Figure 3B).

Additional experiments performed by confocal microscopy showed that, in ISs induced by pDCs, PKC-θ was surrounded by the actin ring as previously described for ISs induced by other APCs, whereas activated Vav was localized throughout the contact zone (Figure 3C). pY174-Vav was also concentrated throughout the IS on cDC–T-cell conjugates (Figure S3C). Western blot analysis confirmed that PKC-θ phosphorylation levels were higher when T cells were activated by mature cDCs, with immature pDCs giving the weakest signal. Similar patterns were found for activation and phosphorylation of Vav and of 2 other molecules involved in T-cell signaling: ζ-chain–associated protein 70 (ZAP-70) and the adaptor molecule linker for the activation of T cells (LAT; Figure 3D). As expected, no significant activation of these signaling molecules was observed in the absence of antigen (Figure S3D; and data not shown).

We then compared the capacity of immature and mature pDCs and cDCs to induce the activation and proliferation of naive OT-II T cells in vitro. Although pDCs and cDCs were able to induce T-cell activation and proliferation, it was evident that immature pDCs showed a diminished stimulatory effect on both CD25 expression and ³H-TdR incorporation (Figure 4A,B). To assess the

possible role of low levels of MHC class II expression by immature pDCs on their diminished immunogenic capability, cell proliferation assays were performed with decreasing concentrations of OVA peptide. Interestingly, similar results to those obtained with a single concentration of OVA peptide were observed (Figure 4C). Furthermore, assays of cell proliferation by carboxyfluorescein diacetate succinimidyl ester dilution confirmed these results, and additional experiments on CD25 induction showed a similar trend (data not shown). These results suggested that factors other than the diminished expression of MHC class II molecules by immature pDCs may also determine the low stimulatory potential of these cells.

Dynamics of CD4⁺ T-cell–pDC interactions in vitro

Because the low immunogenic capacity of immature pDCs could be related to a short duration of their interactions with T cells, we analyzed the dynamics of OT-II T-cell–DC conjugation by time-lapse videomicroscopy. We found that the majority of T-cell interactions with immature pDCs were short-lived (< 5 minutes; Figure 5; Video S1). In contrast, immature cDCs (as well as mature pDCs and cDC) showed a significantly higher proportion of medium-lived (5-15 minutes) and long-lived (> 15 minutes) contacts (Figure 5A,B; Videos S2-S4). Mean contact duration of CD4⁺ T cells with immature pDCs (5.8 minutes ± 1.3 minutes) was significantly lower ($P < .05$) than that with mature pDCs
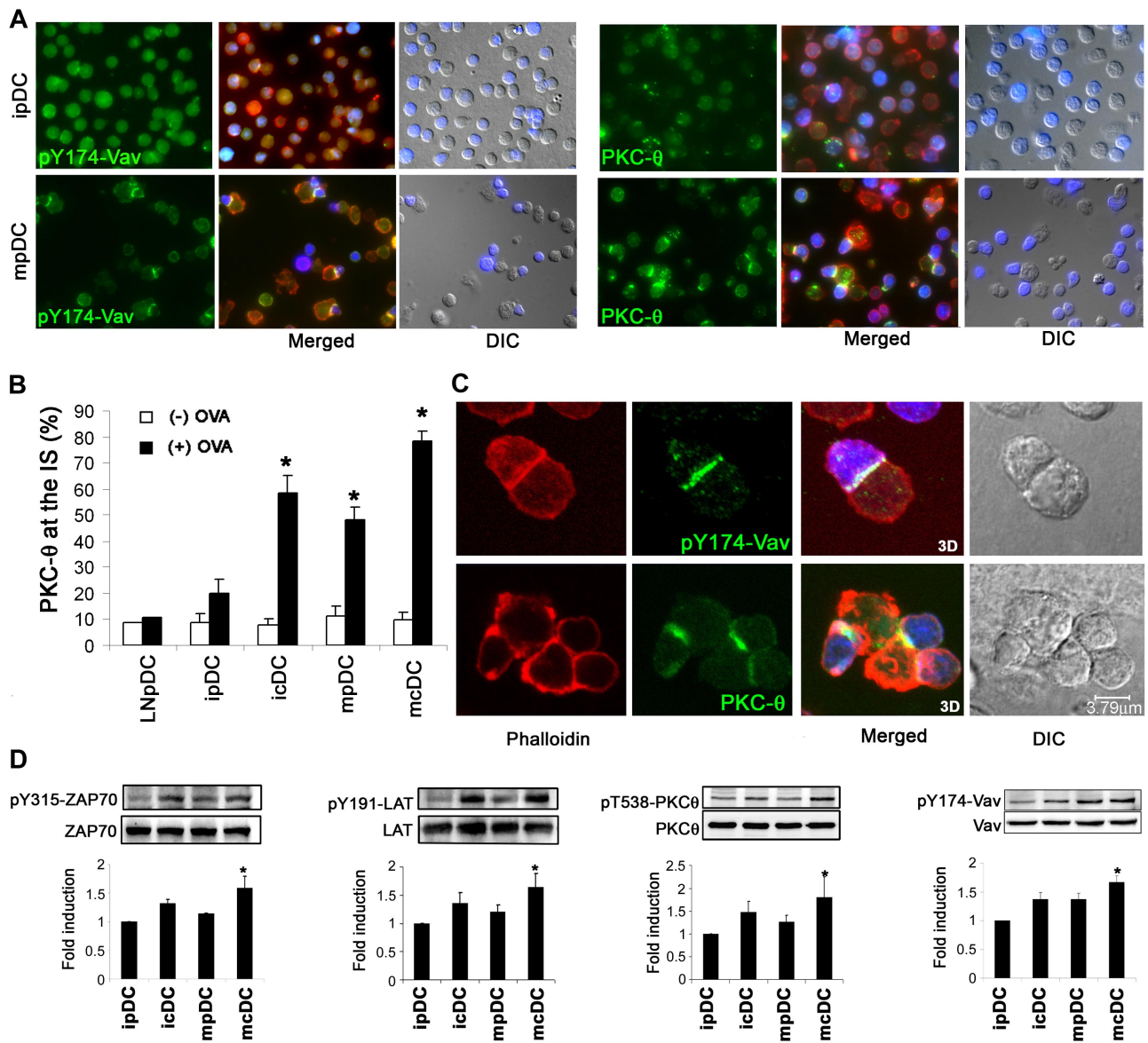
Figure 3. Signaling at the contact zone between plasmacytoid DCs and T lymphocytes. (A) PKC-θ and pY174Vav are relocated to the IS between mature pDCs and T lymphocytes. OVA peptide–loaded immature and mature pDCs were conjugated with blue-labeled OT-II CD4+ T cells and double-stained for pY174-Vav or PKC-θ (green) and phalloidin (red). (B) The chart shows quantification of PKC-θ localization at the IS of immature or mature Flt3-L–derived cDCs and pDCs as well as pDCs isolated from lymph nodes (LNpDC), in either the absence or the presence of OVA peptide. Results are presented as the arithmetic mean plus or minus SEM of PKC-θ contact-zone localization from 5 experiments. *$P < .05$ compared with the absence of antigen. (C) pY174-Vav is localized throughout the pDC–T-cell contact zone, whereas PKC-θ is concentrated at the IS cSMAC and surrounded by actin. pDC–T-cell conjugates were generated in the presence of OVA and double-stained for phalloidin and pY174-Vav or PKC-θ. Plates show a confocal section, the maximal projection of confocal sections, and the differential interference contrast image. (D) Western analysis of ZAP-70, LAT, PKC-θ, and Vav phosphorylation in T cells interacting with immature and mature pDCs and cDCs. One representative experiment is shown of 3 performed. Densitometric analyses were performed, and the ratio between the phosphorylated protein and corresponding total protein expression was determined. Results are expressed as the arithmetic mean plus or minus SD of the fold induction, using as denominator the immature pDC condition, of 3 experiments, and statistical analysis was by the Kruskal-Wallis test (*$P < .05$). ipDC indicates immature pDCs; mpDC, mature pDCs; icDC, immature cDCs; mcDC, mature cDCs.

(16.2 ± 1.1 minutes), immature cDCs (9.7 ± 1.5 minutes), and mature cDCs (24.8 ± 0.9 minutes).

Imaging of pDC-T-cell interactions in vivo

To analyze pDC–T-cell interactions in the physiologic environment of lymphoid organs, we performed intravital 2-photon experiments after adoptive transfer of OVA peptide–loaded immature and mature pDCs and OT-II CD4+ T cells. Because migration of cDCs to lymph nodes has been demonstrated to induce their maturation,[23] we first examined whether immature pDCs were induced to mature after migration. For this, immature Flt3-L–derived pDCs from Ly5.2+ mice were injected intravenously or subcutaneously into

syngeneic Ly5.1+ recipients, and their presence was detected in the spleen and popliteal lymph nodes after 20 hours. Flow cytometric analyses showed that pDCs migrated more efficiently to the spleen than to the popliteal lymph nodes (Figure 6A) and that Ly5.2+ pDCs that had migrated into the popliteal lymph nodes of Ly5.1 mice bore the hallmarks of mature DCs (high expression of MHC class II and CD86 molecules; Figure 6B). In contrast, Ly5.2+ pDCs that had migrated after intravenous injection into the spleen only showed a slight increase in the expression of MHC class II and costimulatory molecules (Figure 6B). Additional flow cytometry analyses showed that, although both immature and mature pDCs were able to induce the activation of Ly5.2+OT-II T cells, as
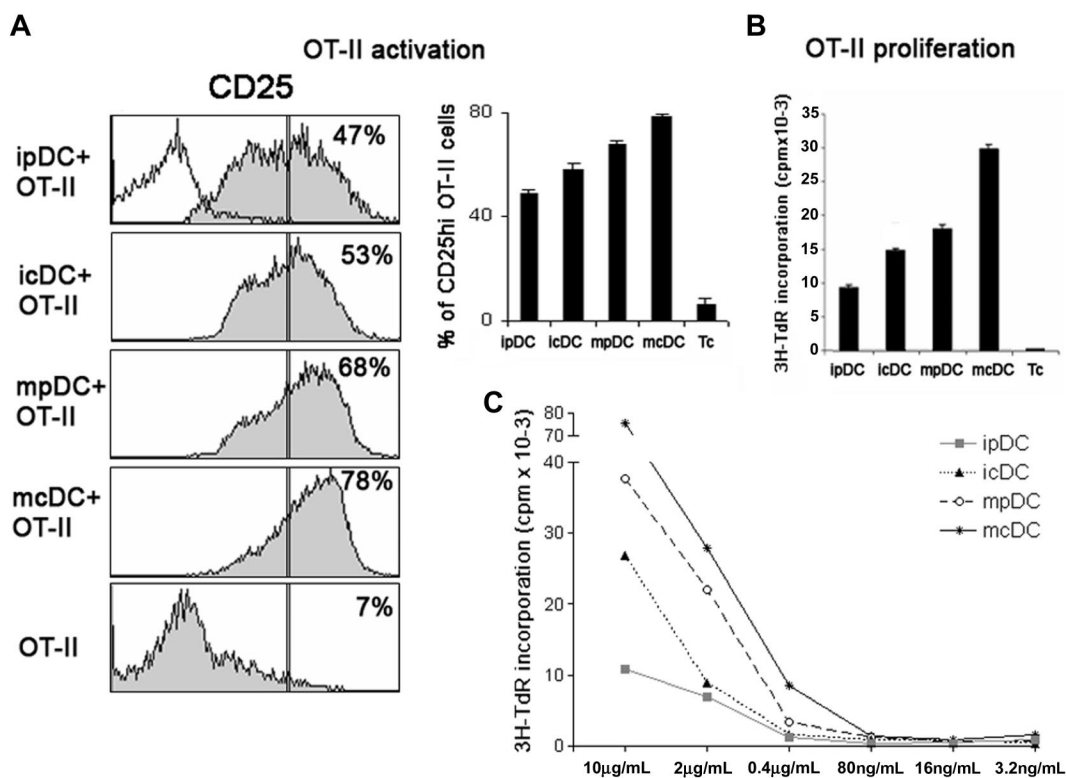
Figure 4. Induction of T-cell activation by pDCs vs cDCs. (A) Immature or mature pDCs and cDCs were cultured with OT-II CD4$^+$ T cells in the presence of OVA peptide (10 μg/mL) for 72 hours, and T-cell CD25 expression was analyzed by flow cytometry. The unfilled histogram shows the negative control. Representative histograms are shown, and statistical analysis is shown in the bar chart. *$P < .05$ compared with immature pDCs by Kruskal-Wallis test. (B) T-cell proliferation was assessed by [^{3}H]thymidine incorporation after 72 hours of culture with DCs. (C) Analysis of cell proliferation by [^{3}H]thymidine incorporation on T cells stimulated by DCs loaded with decreasing concentrations of OVA peptide (10 μg/mL to 3.2 ng/mL) for 72 hours.

assessed by their forward scatter pattern and CD25 expression, the immunogenic capability of immature pDCs was lower than that of mature cells (Figure 6C).

To visualize pDC–T-cell interaction in vivo, immature and mature pDCs derived from GFP transgenic mice and loaded with OVA peptide were injected intravenously into syngeneic C57BL/6 recipients. After 16 hours, OT-II CD4$^+$ cells labeled with the red fluorescent dye CMTMR were injected intravenously into the same recipient. Finally, 4 hours after transfer, mice were anesthetized and the spleen microsurgically exposed for analysis by intravital 2-photon microscopy. This analysis allows imaging up to a depth of 150 μm, corresponding mainly to the red pulp area. Before the 2-photon microscopy, the splenic anatomic compartments in which transferred pDCs and T cells were localized were determined in histologic sections from similarly treated animals. It has been recently reported that, in untreated mice, whereas cDCs are mostly located in the outer T-cell areas and in the marginal zone, with few cDCs in the red pulp, pDCs are mainly located in the red pulp and the T-cell area.[24] We found that the transferred pDCs were preferentially located in the red pulp close to the marginal zone, with a few scattered cells within the white pulp; in contrast, T lymphocytes were mainly concentrated in the T-cell areas, although they were frequently observed in the red pulp, colocalizing with pDCs (Figure 6D). Further analysis revealed that, in the presence of OVA peptide, immature pDCs mainly established short-lived interactions with T cells (< 5 minutes, Figure 6E,F; Video S5). In contrast, a higher proportion of intermediate- and long-lived interactions were observed with mature pDCs (Figure 6E,F; Video S6). These findings are in agreement with our results of in vitro experiments and demonstrate that immature pDCs show

a very limited capability to establish productive interactions with T cells.

Discussion

Although it has been considered that pDCs are mainly involved in innate antiviral responses, recent research has focused on their function in adaptive immunity as professional APCs.[25] In the present study, we have characterized, both in vitro and in vivo, how pDCs physically interact with naive CD4$^+$ T cells.

The precise structure of the IS remains a matter of controversy. Whereas canonical pSMAC-cSMAC patterns have been described in studies of T cell–B cell and T cell–planar bilayer interactions,[26] both multifocal structures and concentric organizations have been reported for T-cell–DC ISs.[27-29] However, it is well established that the DC-actin cytoskeleton plays an active role during IS formation by providing a structural scaffold for several key molecules involved in T-cell activation.[30] Our data show that mature pDCs are able to form canonical IS with CD4$^+$ T cells, with clustering and segregation of key molecules into SMACs, and rearrangement of the actin cytoskeleton and translocation of the T-cell MTOC. The existence of a canonical IS between pDCs and T cells is further supported by the segregation of PKC-θ surrounded by actin cytoskeleton at the pSMAC. Interestingly, a recent report has revealed an essential role for PKC-θ in breaking SMAC symmetry, destabilizing the IS, and determining IS duration.[31] Moreover, we observed that Vav, which has an essential role in T-cell signaling and integrin clustering during antigen presentation,[32] is located throughout the contact zone. In contrast, immature pDCs showed a
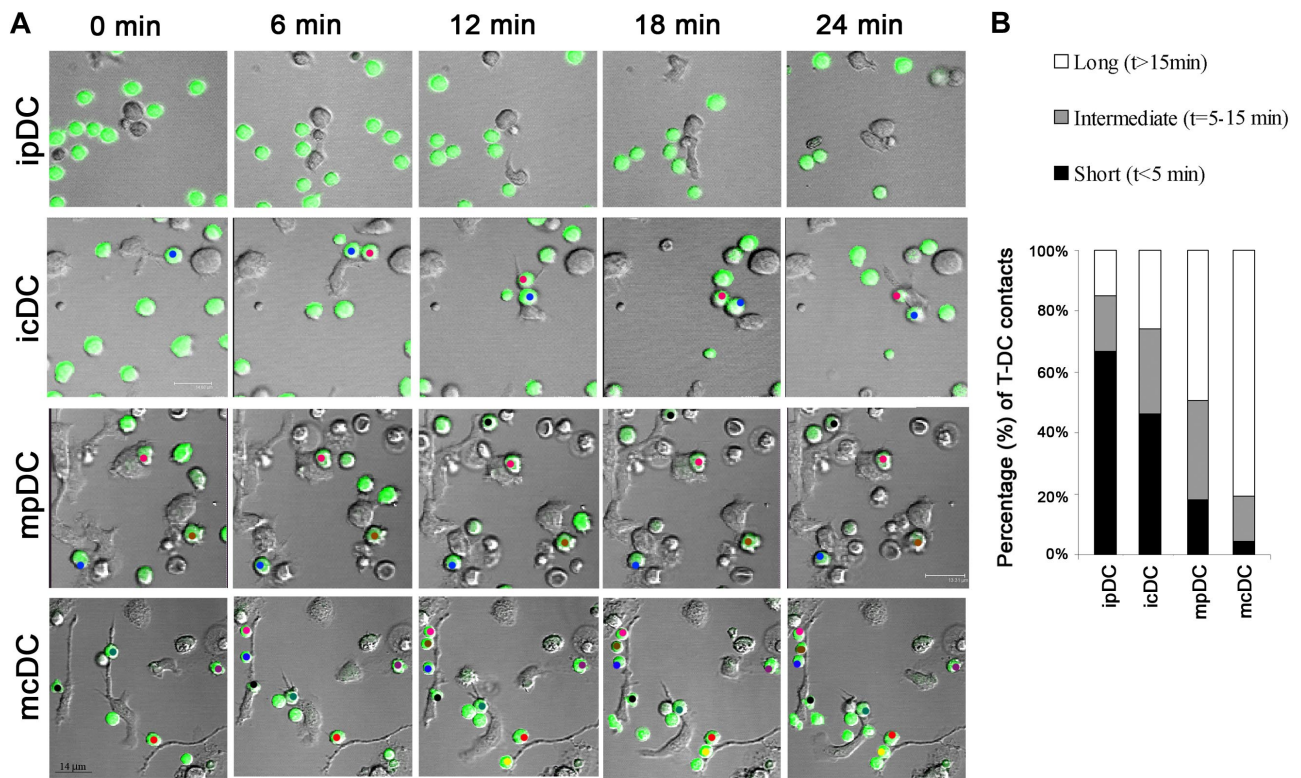
Figure 5. Dynamics of pDC–T-cell interactions. pDCs and cDCs were isolated from Flt3-L-driven cultures. Immature (i) or mature (m) DCs were incubated with OVA peptide and seeded onto fibronectin-coated coverslips. OT-II CD4+ T cells labeled with the green probe calcein were added to the chambers. Contacts between T cells and DCs were monitored by time-lapse videomicroscopy for 30 minutes, and the contact times of individual DC–T-cell pairs were measured. (A) Representative images are shown of different time frames of the video-recorded movies. Each T cell that interacted for more than 15 minutes is marked by a different colored dot. (B) T-cell–DC interactions were classified into 3 categories based on the duration of the interaction: short (< 5 minutes), medium (5-15 minutes), and long (> 15 minutes). Data represent the proportion of each category.

diminished capability to form stable conjugates with T cells as well as a deficient activity as immunogenic APC.

On the basis of previous reports,[33] it can be postulated that the deficient capacity of immature pDCs to form stable interactions with CD4+ T cells is related to a diminished expression of adhesion and/or costimulatory and MHC class II molecules. In this regard, it has been described that peptide-MHC class II potency dictates the duration of cDC–T-cell contacts.[34] We have found that immature pDCs, in contrast to the other DCs analyzed here, expressed very low levels of MHC class II molecules and were inefficient at promoting conjugate formation even in the presence of antigen. Accordingly, these immature cells showed a limited immunogenic capability. However, it is of interest that, despite their very low levels MHC class II expression, immature pDCs were able to induce a modest but significant level of T-cell activation and proliferation.

Our data suggest that ex vivo–isolated pDCs and in vitro-generated pDCs are not completely equivalent, mainly regarding the expression levels of MHC class II molecules. However, we have found that these 2 cell types show a similar behavior in conjugate formation and PKC-θ relocation assays. Moreover, it has been previously described that freshly isolated pDCs exhibit a reduced T-cell stimulatory potential,[5] similar to that described here for in vitro–derived immature pDCs.

Adhesion molecules are essential for scanning the DC surface by T cells during the initial phases of synapse formation.[13,35] Our data indicate that immature pDCs express lower levels of adhesion molecules and integrins than cDCs, and that the surface expression of these molecules is up-regulated after maturation. These differences are especially notable for ICAM-1, and this might partly explain the different capacities to form DC–T-cell conjugates

observed in this study because ICAM-1 expression by DCs is required for long-lasting T-cell–DC contacts.[36]

A striking observation in the present study was the lack of cell surface expression of the tetraspanin CD9 by pDCs, but not by cDCs, irrespective of their maturation state. Tetraspanin microdomains have been proposed as membrane organizers on the basis of their lateral association with several surface receptors, including adhesion and MHC class II molecules.[20] Although tetraspanins are localized at the cSMAC during IS,[37] their precise role in T-APC conjugate formation has not been elucidated. However, it has been described that CD9 enhances the immunogenic capacity of DCs by promoting the formation of MHC class II multimers.[21] Moreover, tetraspanin microdomains are enriched in MHC class II molecules carrying a selected set of peptide antigens, and APCs deficient in tetraspanin microdomains have a reduced capacity to activate CD4+ T cells.[38] Therefore, it is feasible that the lack of expression of CD9 by immature pDCs significantly contributes to their modest capability to induce T-cell activation and proliferation. In addition, the absence of CD9 on the cell membrane of mature pDCs might also be related to their lower immunogenic effect compared with mature cDCs. However, the exact role of CD9 in the formation of the IS and the stimulatory activity of DCs remains as an interesting point to be defined.

Our data show that immature pDCs are less efficient at inducing the activation of signaling molecules and the proliferation of T cells. In this regard, it has been described that defective LAT activation is associated with T-cell anergy.[39] In addition, previous studies have proposed a role for pDCs in the maintenance of peripheral tolerance. Thus, immature thymic pDCs have been reported to promote the differentiation of regulatory T cells in vitro,[5] and lung pDCs prevent in vivo sensitization to inhaled
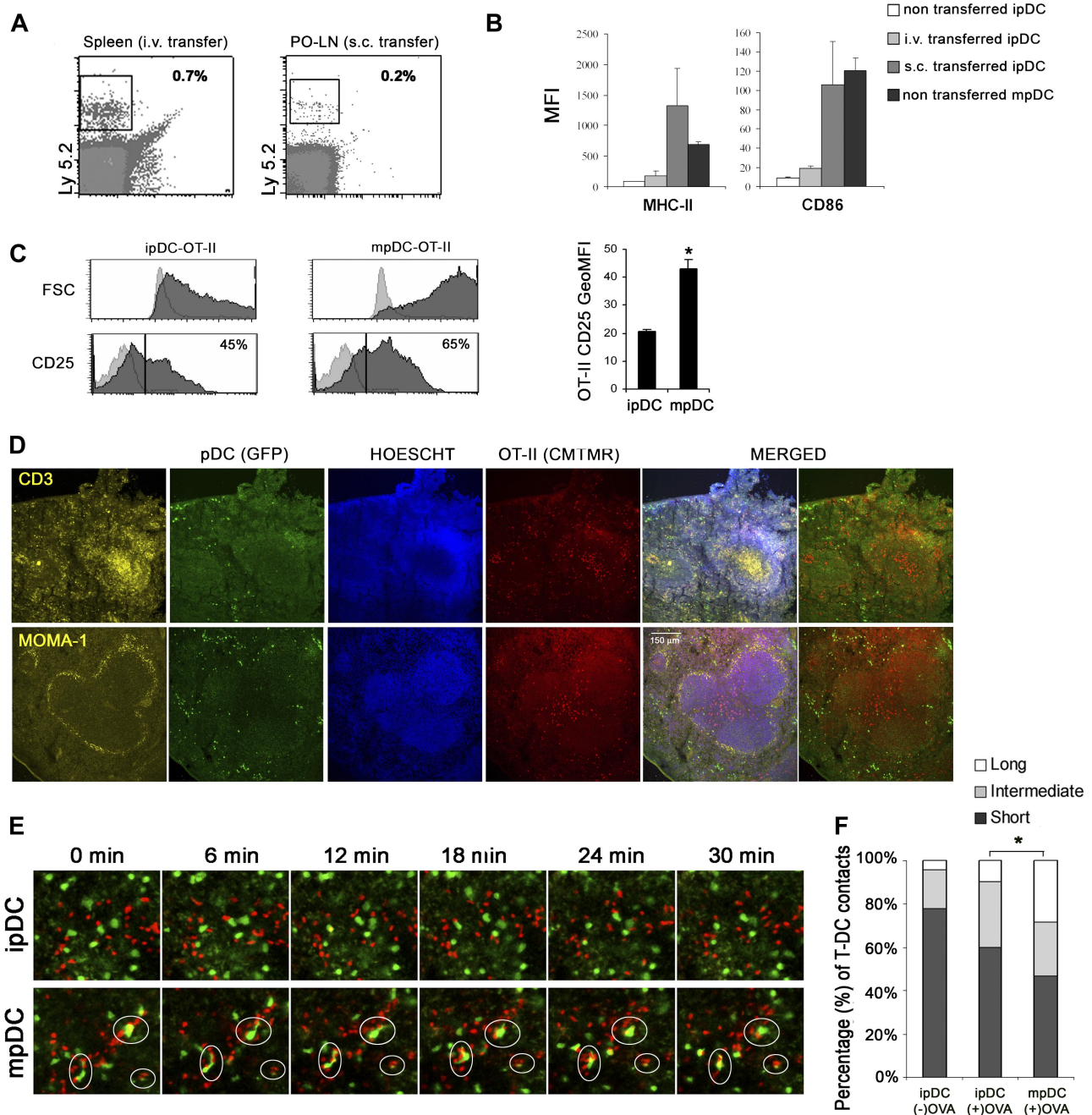
Figure 6. Intravital pDCs and T-cell dynamics. (A) Immature Ly5.2+ Flt3-L–derived pDCs were intravenously or subcutaneously injected into Ly5.1+ mice. After 20 hours, pDCs in spleen or draining popliteal lymph nodes (LN) were analyzed by flow cytometry. Density plots indicate the percentage of Ly5.2+ pDCs that migrated into each lymphoid organ. (B) The bar charts show MHC class II and CD86 expression on immature pDCs before (□) or after intravenous (▨) or subcutaneous injection (▩) and on in vitro–matured (CpG treated) pDCs (■). Data are mean fluorescence intensities (MFI) plus or minus SEM. (C) Mature or immature Ly5.2+ pDCs loaded with OVA peptide and Ly5.2+ OT-II CD4+ T cells were intravenously injected into mice. After 48 hours, the activation of transferred T cells was assessed by forward scatter pattern and CD25 expression (■). Negative controls in which only OT-II CD4+ T cells were injected are overlaid (▨). The chart shows geometric MFI plus or minus SEM of T-cell CD25 expression. *$P < .05$ by Mann-Whitney test. (D) Flt3-L–derived pDCs from GFP mice were intravenously injected into C57BL/6 recipients. After 16 hours, the recipients were intravenously injected with OT-II CD4+ cells labeled with CMTMR. After 4 hours, mice were killed and spleen sections were stained for CD3 or MOMA-1 (yellow) and Hoechst for nuclear staining (blue). Plates show maximal projections of confocal sections. (E) pDCs from GFP mice were either left immature or matured with CpG (24 hours) and then loaded as indicated with OVA peptide and intravenously injected into C57BL/6 recipients. After 16 hours, the recipients were intravenously injected with OT-II CD4+ cells labeled red with CMTMR. Mice were anesthetized 4 hours later and spleens were microsurgically exposed for intravital 2-photon imaging. Intravital time-lapse 2-photon laser scanning microscopy images of GFP (pDCs) and CMTMR-labeled T cells (red) are presented as average intensity projections along the z-axis. Long-lasting interactions are indicated (circles). Images were average-projected using ImageJ (National Institutes of Health), and manual tracking of individual cells was performed with Metamorph software. (F) DC–T-cell interactions were classified into 3 categories according to their duration: short (< 5 minutes), medium (5-15 minutes), and long (> 15 minutes). The histogram shows the proportions in each category. *$P < .05$ compared with immature pDCs by χ^2 test. Results represent more than 100 interactions per condition from duplicates from 2 independent experiments (n = 144 for ipDCs [−OVA], n = 212 for ipDCs [+OVA], and n = 109 for mpDCs [+ OVA]).

antigens.[12] Furthermore, an essential role has been demonstrated for pDCs during the induction of regulatory T cells in transplant tolerance,[10] tumor immunology,[40] and autoimmune diseases.[41]

The contributions made by DC–T-cell contact duration and frequency to the functional T-cell outcome remain a matter of debate. Our results demonstrate that mature pDCs preferentially establish long-lived

DC–T-cell interactions, whereas immature pDCs mainly form short-lived interactions. The importance of prolonged T-cell–DC interactions for efficient CD4^{+} T-cell activation in vivo has been recently reported.[42] Other studies have revealed that, under experimental conditions leading to CD8^{+} T-cell tolerance, CD8^{+} T cells failed to establish long-lasting contacts with DCs and, instead, made multiple short-lived contacts.[43] However, other studies have demonstrated that, although only a low percentage of T cells are arrested under tolerogenic conditions, the overall T-cell mean velocity was similar both under priming and under tolerogenic conditions.[44,45] In the case of pDCs, we consider that additional studies are necessary to elucidate the functional consequence of short-lived contacts between pDC and T cells and whether or not there exists a causal relationship among maturation state of the pDC, contact duration, and immunogenic function.

In conclusion, our work describes the characteristics and dynamics of cell-cell interactions between pDCs and CD4^{+} T lymphocytes and explores their functional consequences. Our data indicate that immature pDCs preferentially form transitory contacts with naive T cells, and exhibit a very limited capability to induce the activation of these cells. Our study also suggests that, on maturation, pDCs can function as professional APCs, establishing long-lived stable contacts with T cells, forming functional ISs able to initiate T-cell activation.

Acknowledgments

Authorship

Contribution: M.M., G.M.d.H., C.A., and F.S.-M. conceived and designed the experiments; M.M., G.M.d.H., M.L.-B., N.B.M.-C., L.F., and A.S. performed experiments and analyzed data; S.H. and S.A. contributed materials/analysis tools and had scientific discussion; and M.M., G.M.d.H., C.A., and F.S.-M. wrote the paper and had extensive scientific discussion for this study.

Conflict-of-interest disclosure: The authors declare no competing financial interests.

Correspondence: Francisco Sánchez-Madrid, Departamento de Biología Vascular e Inflamación, Centro Nacional de Investigaciones Cardiovasculares, Melchor Fernández Almagro 3, 28029 Madrid, Spain; e-mail: fsanchez.hlpr@salud.madrid.org.

References

1. Banchereau J, Steinman RM. Dendritic cells and the control of immunity. Nature. 1998;392:245-252.

2. Colonna M, Trinchieri G, Liu YJ. Plasmacytoid dendritic cells in immunity. Nat Immunol. 2004;12:1219-1226.

3. Nakano H, Yanagita M, Gunn MD. CD11c(+)B220(+)Gr-1(+) cells in mouse lymph nodes and spleen display characteristics of plasmacytoid dendritic cells. J Exp Med. 2001;194:1171-1178.

4. Asselin-Paturel C, Boonstra A, Dalod M, et al. Mouse type I IFN-producing cells are immature APCs with plasmacytoid morphology. Nat Immunol. 2001;2:1144-1150.

5. Martin P, Del Hoyo GM, Anjuere F, et al. Characterization of a new subpopulation of mouse CD8alpha+ B220+ dendritic cells endowed with type 1 interferon production capacity and tolerogenic potential. Blood. 2002;100:383-390.

6. Barchet W, Cella M, Colonna M. Plasmacytoid dendritic cells: virus experts of innate immunity. Semin Immunol. 2005;17:253-261.

7. Hoeffel G, Ripoche AC, Matheoud D, et al. Antigen crosspresentation by human plasmacytoid dendritic cells. Immunity. 2007;27:481-492.

8. Lande R, Gregorio J, Facchinetti V, et al. Plasmacytoid dendritic cells sense self-DNA coupled with antimicrobial peptide. Nature. 2007;449:564-569.

9. Ito T, Yang M, Wang YH, et al. Plasmacytoid dendritic cells prime IL-10-producing T regulatory cells by inducible costimulator ligand. J Exp Med. 2007;204:105-115.

10. Ochando JC, Homma C, Yang Y, et al. Alloantigen-presenting plasmacytoid dendritic cells mediate tolerance to vascularized grafts. Nat Immunol. 2006;7:652-662.

11. Jonuleit H, Schmitt E, Steinbrink K, Enk AH. Dendritic cells as a tool to induce anergic and regulatory T cells. Trends Immunol. 2001;22:394-400.

12. de Heer HJ, Hammad H, Soullie T, et al. Essential role of lung plasmacytoid dendritic cells in preventing asthmatic reactions to harmless inhaled antigen. J Exp Med. 2004;200:89-98.

13. Montoya MC, Sancho D, Bonello G, et al. Role of ICAM-3 in the initial interaction of T lymphocytes and APCs. Nat Immunol. 2002;3:159-168.

14. Dustin ML. A novel adaptor protein orchestrates receptor patterning and cytoskeletal polarity in T-cell contacts. Cell. 1998;94:667-677.

15. Monks CRF, Freiberg BA, Kupfer H, Sclaky N, Kupfer A. Three-dimensional segregation of supramolecular activation clusters in T cells. Nature. 1998;395:82-86.

16. Varma R, Campi G, Yokosuka T, Saito T, Dustin ML. T cell receptor-proximal signals are sustained in peripheral microclusters and terminated in the central supramolecular activation cluster. Immunity. 2006;25:117-127.

17. Martin-Cofreces NB, Sancho D, Fernandez E, et al. Role of Fyn in the rearrangement of tubulin cytoskeleton induced through TCR. J Immunol. 2006;176:4201-4207.

18. Brawand P, Fitzpatrick DR, Greenfield BW, Brasel K, Maliszewski CR, De Smedt T. Murine plasmacytoid pre-dendritic cells generated from Flt3 ligand-supplemented bone marrow cultures are immature APCs. J Immunol. 2002;169:6711-6719.

19. Gilliet M, Boonstra A, Paturel C, et al. The development of murine plasmacytoid dendritic cell precursors is differentially regulated by FLT3-ligand and granulocyte/macrophage colony-stimulating factor. J Exp Med. 2002;195:953-958.

20. Hemler ME. Tetraspanin functions and associated microdomains. Nat Rev Mol Cell Biol. 2005;6:801-811.

21. Unternaehrer JJ, Chow A, Pypaert M, Inaba K, Mellman I. The tetraspanin CD9 mediates lateral association of MHC class II molecules on the dendritic cell surface. Proc Natl Acad Sci U S A. 2007;104:234-239.

22. Sancho D, Vicente-Manzanares M, Mittelbrunn M, et al. Regulation of microtubule-organizing center orientation and actomyosin cytoskeleton rearrangement during immune interactions. Immunol Rev. 2002;189:84-97.

23. Bonasio R, von Andrian UH. Generation, migration and function of circulating dendritic cells. Curr Opin Immunol. 2006;18:503-511.

24. Asselin-Paturel C, Brizard G, Chemin K, et al. Type I interferon dependence of plasmacytoid dendritic cell activation and migration. J Exp Med. 2005;201:1157-1167.

25. Liu YJ. IPC: professional type 1 interferon-producing cells and plasmacytoid dendritic cell precursors. Annu Rev Immunol. 2005;23:275-306.

26. Dustin ML, Tseng SY, Varma R, Campi G. T cell-dendritic cell immunological synapses. Curr Opin Immunol. 2006;18:512-516.

27. Brossard C, Feuillet V, Schmitt A, et al. Multifocal structure of the T cell-dendritic cell synapse. Eur J Immunol. 2005;35:1741-1753.

28. de la Fuente H, Mittelbrunn M, Sanchez-Martin L, et al. Synaptic clusters of MHC class II molecules induced on DCs by adhesion molecule-mediated initial T-cell scanning. Mol Biol Cell. 2005;16:3314-3322.

29. Rothoeft T, Balkow S, Krummen M, et al. Structure and duration of contact between dendritic cells and T cells are controlled by T-cell activation state. Eur J Immunol. 2006;36:3105-3117.

30. Al-Alwan MM, Rowden G, Lee TD, West KA. The dendritic cell cytoskeleton is critical for the formation of the immunological synapse. J Immunol. 2001;166:1452-1456.

31. Sims TN, Soos TJ, Xenias HS, et al. Opposing effects of PKCtheta and WASp on symmetry breaking and relocation of the immunological synapse. Cell. 2007;129:773-785.

32. Tybulewicz VL. Vav-family proteins in T-cell signalling. Curr Opin Immunol. 2005;17:267-274.

33. Benvenuti F, Lagaudriere-Gesbert C, Grandjean I, et al. Dendritic cell maturation controls adhesion, synapse formation, and the duration of the interactions with naive T lymphocytes. J Immunol. 2004;172:292-301.

34. Skokos D, Shakhar G, Varma R, et al. Peptide-MHC potency governs dynamic interactions between T cells and dendritic cells in lymph nodes. Nat Immunol. 2007;8:835-844.

35. Lebedeva T, Dustin ML, Sykulev Y. ICAM-1 costimulates target cells to facilitate antigen presentation. Curr Opin Immunol. 2005;17:251-258.

36. Scholer A, Hugues S, Boissonnas A, Fetler L, Amigorena S. Intercellular adhesion molecule-1-dependent stable interactions between T cells and dendritic cells determine CD8+ T cell memory. Immunity. 2008;28:258-270.

37. Mittelbrunn M, Yanez-Mo M, Sancho D, Ursa A, Sanchez-Madrid F. Cutting edge: dynamic redistribution of tetraspanin CD81 at the central zone of the immune synapse in both T lymphocytes and APC. J Immunol. 2002;169:6691-6695.

38. Kropshofer H, Spindeldreher S, Rohn TA, et al. Tetraspan microdomains distinct from lipid rafts enrich select peptide-MHC class II complexes. Nat Immunol. 2002;3:61-68.

39. Hundt M, Tabata H, Jeon MS, et al. Impaired activation and localization of LAT in anergic T cells as a consequence of a selective palmitoylation defect. Immunity. 2006;24:513-522.

40. Sharma MD, Baban B, Chandler P, et al. Plasmacytoid dendritic cells from mouse tumor-draining lymph nodes directly activate mature Tregs via indoleamine 2,3-dioxygenase. J Clin Invest. 2007;117:2570-2582.

41. Kang HK, Liu M, Datta SK. Low-dose peptide tolerance therapy of lupus generates plasmacytoid dendritic cells that cause expansion of autoantigen-specific regulatory T cells and contraction of inflammatory Th17 cells. J Immunol. 2007;178:7849-7858.

42. Celli S, Lemaitre F, Bousso P. Real-time manipulation of T cell-dendritic cell interactions in vivo reveals the importance of prolonged contacts for CD4(+) T-cell activation. Immunity. 2007;27:625-634.

43. Hugues S, Fetler L, Bonifaz L, Helft J, Amblard F, Amigorena S. Distinct T cell dynamics in lymph nodes during the induction of tolerance and immunity. Nat Immunol. 2004;5:1235-1242.

44. Shakhar G, Lindquist RL, Skokos D, et al. Stable T cell-dendritic cell interactions precede the development of both tolerance and immunity in vivo. Nat Immunol. 2005;6:707-714.

45. Zinselmeyer BH, Dempster J, Gurney AM, et al. In situ characterization of CD4+ T cell behavior in mucosal and systemic lymphoid tissues during the induction of oral priming and tolerance. J Exp Med. 2005;201:1815-1823.